

Contents lists available at [SciVerse ScienceDirect](http://www.sciencedirect.com)

Chemical Engineering Journal

journal homepage: [www.elsevier.com/locate/cej](http://www.elsevier.com/locate/cej)Chemical  
Engineering  
Journal

## Electrochemical reduction behavior of a highly porous SIMFUEL particle in a LiCl molten salt

Eun-Young Choi<sup>a</sup>, Jae Won Lee<sup>a</sup>, Jang Jin Park<sup>a</sup>, Jin-Mok Hur<sup>a</sup>, Jong-Kook Kim<sup>a</sup>, Kyeong Youl Jung<sup>b</sup>, Sang Mun Jeong<sup>c,\*</sup>

<sup>a</sup> Korea Atomic Energy Research Institute, Yuseong-gu, Daejeon 305-353, Republic of Korea

<sup>b</sup> Department of Chemical Engineering, Kongju National University, Cheonan, Chungnam 330-717, Republic of Korea

<sup>c</sup> Department of Chemical Engineering, Chungbuk National University, Cheongju, Chungbuk 361-763, Republic of Korea

### HIGHLIGHTS

- ▶ A highly porous SIMFUEL particle was prepared as a feed material for electrochemical reduction.
- ▶ Cathodic and anodic behaviors of the particles were observed.
- ▶ The porous structure can speed up the electrochemical reduction.
- ▶ The porous structure is helpful to achieve a high reduction extent of each element.

### ARTICLE INFO

#### Article history:

Available online xxxxx

#### Keywords:

Pyroprocessing  
SIMFUEL particle  
Molten salt  
Electrochemical reduction  
Reduction extent

### ABSTRACT

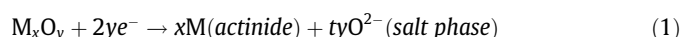
A highly porous SIMFUEL particle is prepared here for use as a feed material for electrochemical reduction. The prepared particles were found to have highly porous and sintered structure. The particles were electrolyzed in a LiCl-1 wt.% Li<sub>2</sub>O melt at 650 °C. A steel basket containing the particles and a platinum plate were used as a cathode and an anode, respectively. The analysis result reveals the reduction extent of uranium oxide to be in excess of 99%. The rare earth oxides were reduced to their metallic form in the range of 46–78%. The highly porous structure of the SIMFUEL particles is advantageous to speed up the electrochemical reduction process for pyroprocessing.

© 2012 Elsevier B.V. All rights reserved.

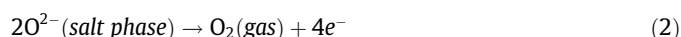
### 1. Introduction

Pyroprocessing technology based on molten salt electrolysis has attracted much attention for the treatment and recycling of metallic or oxide spent fuels owing to benefits, such as its inherent proliferation resistance, the compactness of the process equipment, and the relatively low cost [1–10]. The pyroprocessing involves the reduction of spent oxide fuel to a metal through an electrochemical reduction process and the recovery of the fuel components by means of an electro-refining process [11].

In the electrochemical reduction process, oxides fuels are loaded at the cathode in molten LiCl containing Li<sub>2</sub>O so as to dissolve oxide ions. The overall cathode reaction is as follows [12]:



When a platinum anode is employed, oxygen ions are oxidized to produce oxygen gas on the anode surface, as follows:



When an electrical potential is applied, the actinide metal oxide is reduced to metal and remains at the cathode. The oxygen ion (O<sup>2-</sup>) produced at the cathode is transported through the salt and discharges at the anode to form O<sub>2</sub> gas. Li<sub>2</sub>O is initially added to molten LiCl to speed up the electrochemical reaction and prevent anodic dissolution of platinum. The diffusion of O<sup>2-</sup> ions from the inside of the oxide fuel to the bulk salt significantly affects the reduction rate and current efficiency during electrolysis [13–17]. Because the original spent oxide fuel is too dense and large to achieve high current efficiency, the use of a fine powder, U<sub>3</sub>O<sub>8</sub> prepared via oxidative decladding at ~500 °C has been proposed. In spite of the complete electrochemical reduction from U<sub>3</sub>O<sub>8</sub> to U metal, the handling of U<sub>3</sub>O<sub>8</sub> powder, the use of a thick cathode basket and a significant decrease in the Li<sub>2</sub>O concentration in the bulk electrolyte remain as formidable challenges that must be overcome [9,10]. In more recent reports [18,19], successful trials were described which used porous UO<sub>2</sub> pellet as a feed material for an

\* Corresponding author. Tel.: +82 43 261 3369; fax.: +82 43 269 2370.

E-mail address: [smjeong@chungbuk.ac.kr](mailto:smjeong@chungbuk.ac.kr) (S.M. Jeong).

electrochemical reduction. The powerful benefits of the porous  $\text{UO}_2$  pellet relative to  $\text{U}_3\text{O}_8$  powder include an insignificant decrease in  $\text{Li}_2\text{O}$  concentration in the bulk electrolyte and easy handling due to its appropriate size, shape and density. The preparation of porous  $\text{UO}_2$  pellets consists of five steps: mixing the  $\text{U}_3\text{O}_8$  powder with a lubricant, pressing the mixture into green pellets under a high pressure, calcining the green pellets for the removal of the lubricant at  $\sim 700^\circ\text{C}$ , sintering them at  $1300\text{--}1700^\circ\text{C}$  and finally converting  $\text{UO}_{2+x}$  to  $\text{UO}_2$  by a 4%  $\text{H}_2/\text{Ar}$  gas treatment. Inspired by laborious preparation procedures necessary to create porous  $\text{UO}_2$  pellets, we proposed two-step-approach to produce porous  $\text{UO}_2$  particles via the sintering and rotation of  $\text{U}_3\text{O}_8$  powder at  $\sim 1200^\circ\text{C}$  in a rotary chamber followed by conversion from  $\text{UO}_{2+x}$  to  $\text{UO}_2$  by a 4%  $\text{H}_2/\text{Ar}$  gas treatment. We demonstrated that the density and porosity of  $\text{UO}_2$  particles can be controlled via the rotational speed, sintering temperature and time [20].

Here, a follow-up study was performed to prepare synthesized spent oxide fuel, known as SIMFUEL (simulated high burn-up nuclear fuel) in the form of porous particles. SIMFUEL consists mainly of  $\text{UO}_2$ , but Sr, Y, Zr, Mo, Ru, Rh, Pd, Ba, La, Ce and Nd are added in different amounts depending on which burn-up process is being mimicked. Chemically, SIMFUEL is similar to real spent fuel, but it does not contain radioactive isotopes. In this work, we place particular emphasis on demonstrating the application of porous SIMFUEL particles to the electrochemical reduction process and on evaluating its performance.

## 2. Experimental

### 2.1. Preparation and characterization of the highly porous SIMFUEL particles

Fifteen elements of fission product in spent oxide fuel and the composition of their surrogated oxides for this study are listed in Table 1. The composition is based on an equivalent burn-up of 60,000 MWd/tU (megawatt-days/metric ton of uranium). The surrogated oxides were milled using a mortar and were mixed with  $\text{UO}_2$  powder in a tubular-type mixer. Wet-attrition milling for 4 h led to the creation of a homogeneous powder mixture. This was then pressed at 300 MPa and sintered at  $1700^\circ\text{C}$  for 6 h in an atmosphere of 4%  $\text{H}_2/\text{Ar}$ . The characteristics of this product are described in the previous publication [21]. The SIMFUEL powder was then obtained by vol-oxidation of the pressed mixture at  $500^\circ\text{C}$  for 5 h in an air atmosphere. Next, the SIMFUEL powder was heated to  $700^\circ\text{C}$  at a heat-up rate of  $5^\circ\text{C}/\text{min}$  and maintained at that temperature for 3 h in a rotary vol-oxidizer under an air atmosphere. Next, the rotary vol-oxidizer was filled with high-purity argon gas and the powder was heated and kept at  $1100^\circ\text{C}$  for 3 h under an argon atmosphere, after which it was cooled to room temperature. During the entire heating period, the rotary vol-oxidizer was operated at 3 rpm. The porous particles of SIMFUEL, whose main phase consisted of  $\text{U}_3\text{O}_8$ , were obtained after cooling. Finally, the SIMFUEL particles with  $\text{UO}_2$  as its main phase were achieved after a 4%  $\text{H}_2/\text{Ar}$  gas treatment for 5 h at  $1200^\circ\text{C}$  in a tube furnace. The bulk density and apparent porosity of the SIMFUEL particles were determined by a water immersion method (ASTM-C830-00). The crystalline structure of the SIMFUEL was analyzed by X-ray diffraction (XRD, Rigaku Mini-Flex), and a scanning electron microscopy (SEM, JEOL, JSM-6300) was employed to observe the microstructure.

### 2.2. Electrochemical reduction of the porous SIMFUEL particles

The experimental setup for the electrochemical reduction process is shown in Fig. 1. First, 380 g of  $\text{LiCl}$  was put in the  $\text{MgO}$

**Table 1**  
Chemical composition and surrogated oxides added to  $\text{UO}_2$  powder as fission products.

Impurity groups	Elements in SIMFUEL	Surrogate oxides	Element composition <sup>a</sup> (wt.%)
	U	$\text{UO}_2$	94.459
Dissolved oxides	Y	$\text{Y}_2\text{O}_3$	0.084
	La	$\text{La}_2\text{O}_3$	0.226
	Ce (Pu, Np) <sup>b</sup>	$\text{CeO}_2$	1.342
	Nd (Pr, Sm) <sup>b</sup>	$\text{Nd}_2\text{O}_3$	1.111
	SUM		2.763
Dissolved oxides/oxide precipitates	Sr	$\text{SrO}$	0.150
	Zr	$\text{ZrO}_2$	0.667
	Ba	$\text{BaCO}_3$	0.326
	SUM		1.143
Metallic precipitates	Mo	$\text{MoO}_3$	0.624
	Ru (Tc) <sup>b</sup>	$\text{RuO}_2$	0.566
	Rh	$\text{Rh}_2\text{O}_3$	0.064
	Pd	$\text{PdO}$	0.290
	SUM		1.544
	Oxide/metallic precipitates	Te	$\text{TeO}_2$

<sup>a</sup> With 60,000 MWd/tU burnup and 5 years of cooling.

<sup>b</sup> Element in parenthesis was replaced by the element in the front of parenthesis.

crucible at room temperature. The reactor was heated up and maintained at  $650^\circ\text{C}$ . Then, 3.8 g of  $\text{Li}_2\text{O}$  was fed into the reactor to reach the desired concentration. After complete dissolution of  $\text{Li}_2\text{O}$ , the electrodes were lowered into the molten salt. Bare nickel wire (0.5 mm in diameter) or a porous SIMFUEL particle of 40 mg wound with nickel wire was used as a working electrode for cyclic voltammetry (CV) to investigate its reduction behavior. Also, platinum wire (1 mm in diameter and 10 mm in depth) was used to determine the electrochemical behavior of the  $\text{O}^{2-}$  ions in the molten salt. In the electrochemical reduction test, the cathode basket (18 mm in diameter) was surrounded with a 325 mesh sheet (sieve opening of 45  $\mu\text{m}$  in size) to contain the SIMFUEL particles. A stainless steel rod of 3 mm in diameter was placed in the center of the cathode basket as a current collector. A platinum plate (10 mm

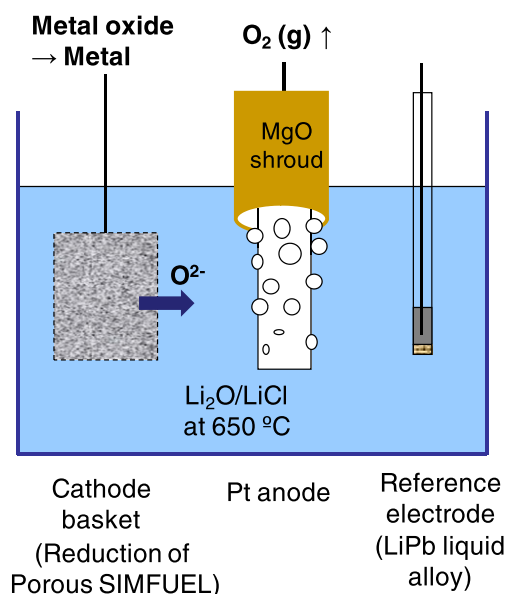


**Fig. 1.** Schematic drawing of the electrochemical reduction process for the SIMFUEL particles.

width  $\times$  30 mm length) and liquid Li–Pb as an alloy (32 mol% Li) were employed as the anode and reference electrode, respectively. Tantalum wire of 0.5 mm as an electrical lead was immersed in the liquid alloy, which was then put into a magnesia tube with a porous bottom. The distance between cathode and anode centers was 30 mm. The porous SIMFUEL particles were electrolyzed by controlling a constant cell voltage with a DC power supply (E3633A, Agilent). During the electrolysis of the porous SIMFUEL particles, the voltage was interrupted intermittently to measure the open circuit potential (OCP) of the cathode. The cathode potential against Li–Pb was monitored during the electrochemical reduction process with a digital multimeter. After an experimental run, the reduction extent of each element was determined by an analysis technique to separate the metal and oxide phases of an electrochemically reduced fuel sample. The phase separation of metal and oxide phases in the oxide mixture was accomplished by contacting the mixture with elemental bromine in an ethyl acetate medium. The metal was dissolved by bromine, leaving the oxide compounds in an insoluble solid phase. The insoluble oxide phase was separated from the dissolved metal phase via centrifuge, decanting and multiple washing steps. After that, the elemental analysis was performed by Inductively Coupled Plasma-Atomic Emission Spectroscopy (ICP-AES). The analysis technique is also described elsewhere [22,23].

### 3. Results and discussion

#### 3.1. Characterization of the porous SIMFUEL particles

Fig. 2a shows an image of the prepared porous SIMFUEL particles. The SIMFUEL powders were collided and aggregated while

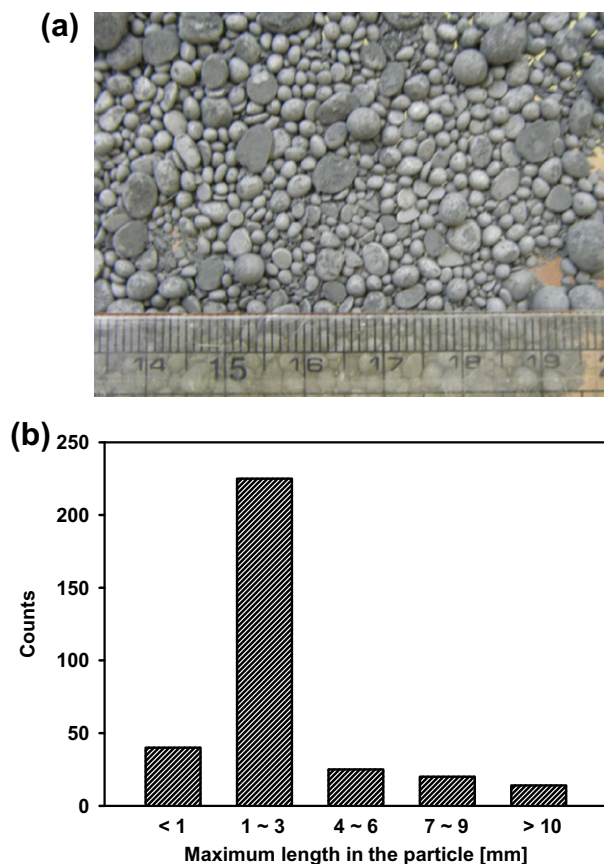


Fig. 2. (a) Photograph of the prepared SIMFUEL particles and (b) its size distribution.

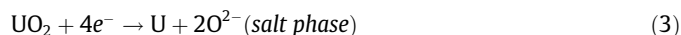
they rolled and/or slumped in the heated rotary voloxidizer, which resulted in round-edge and rice ball-like shape. Its size distribution was analyzed and this result is shown in Fig. 2b. Its size is ranged from 1 to 12 mm. The size of most particles was 1–3 mm. The measured porosity of the prepared porous SIMFUEL particles is 70.7%, which stands in contrast to those of commercial fuel (<5%) or porous  $\text{UO}_2$  pellets (30–45%) [18,19,21]. The density of the SIMFUEL after the thermal process in rotary voloxidizer at 1100 °C was 2.69 g/cm<sup>3</sup> while the density after the 4%– $\text{H}_2$ /Ar gas treatment at 1200 °C was 3.10 g/cm<sup>3</sup> due to the transformation of the main component,  $\text{U}_3\text{O}_8$  (theoretical density TD of 8.4 g/cm<sup>3</sup>) to  $\text{UO}_2$  (TD of 10.96 g/cm<sup>3</sup>).

Microstructures of the SIMFUEL were observed by means of SEM. As presented in Fig. 3e, the SIMFUEL powders were well dispersed with sharp edges. After sintering the SIMFUEL powder while rotating it at 1100 °C, the formation of a neck between grains with round edges, followed by bonding with neighboring grains and grain growth was observed (Fig. 3b). The grains after the 4%– $\text{H}_2$ /Ar gas treatment at 1200 °C, are more sintered, as shown in Fig. 3d. The primary particles, about 5 μm in size, were well-sintered and agglomerated after the treatment. As shown in Fig. 3a and c, cracks did not occur in spite of the dramatic density change, which reflects the physically stable transformation.

The XRD pattern of the prepared porous SIMFUEL particles is shown in Fig. 4b, corresponding to the  $\text{UO}_2$  peak. The patterns of the SIMFUEL before the 4%– $\text{H}_2$ /Ar gas treatment show  $\text{U}_3\text{O}_8$  and  $\text{U}_4\text{O}_9$  (Fig. 4a). This change reflects that  $\text{UO}_2$  as the major phase was successfully achieved via the 4%– $\text{H}_2$ /Ar gas treatment. The characteristic peaks of the other constituents in the XRD result could not be found due to their low content levels in the particles.

#### 3.2. Cyclic voltammetry

Fig. 5a shows the CV curves of a SIMFUEL particle with the number of potential scans in the 1 wt.%  $\text{Li}_2\text{O}/\text{LiCl}$  salt at 650 °C. The cathodic current rises at –0.49 V vs. LiPb, which is most likely related to the electrochemical reduction of  $\text{UO}_2$  according to the following reaction:



Thereafter, a sharp increase in the reduction current takes place due to the deposition of lithium metal from  $\text{Li}^+$  ion in the salt phase. The cathodic current seems to consist of some waves. It is highly probable that these waves of the cathodic current are attributed to the electrochemical reduction of other metal oxides in the SIMFUEL particles. Unfortunately, it is very hard to identify the reduction potential of each metal oxide because the peaks can be overlapped. When the potential scan is reversed, the sharp re-oxidation peak related to the dissolution of the deposited lithium metal and an anodic wave at –0.30 V appear in the first scan. The anodic wave may be due to the re-oxidation of the reduced uranium metal to uranium oxide. The intensity of the re-oxidation peak is reduced as the number of scans increases, suggesting a decrease in the amount of deposited lithium metal [24]. To investigate the anodic behavior during the electrochemical reduction process, a platinum wire was employed as a working electrode for the CV measurement. Fig. 5b shows the CV results of the platinum wire in 0.2 wt.%  $\text{Li}_2\text{O}$ –LiCl at four different scanning ranges. In the scan range of 1.00–2.12 V vs. LiPb, an oxidation peak (a) was observed at 2.06 V due to the formation of  $\text{Li}_2\text{PtO}_3$  [13,25]:



Two cathodic waves (a') were observed in the reverse scan, which implies a two-step reduction of  $\text{Li}_2\text{PtO}_3$ . In a scan up to 2.32 V, an increase in the anodic current (b) and the cathodic wave



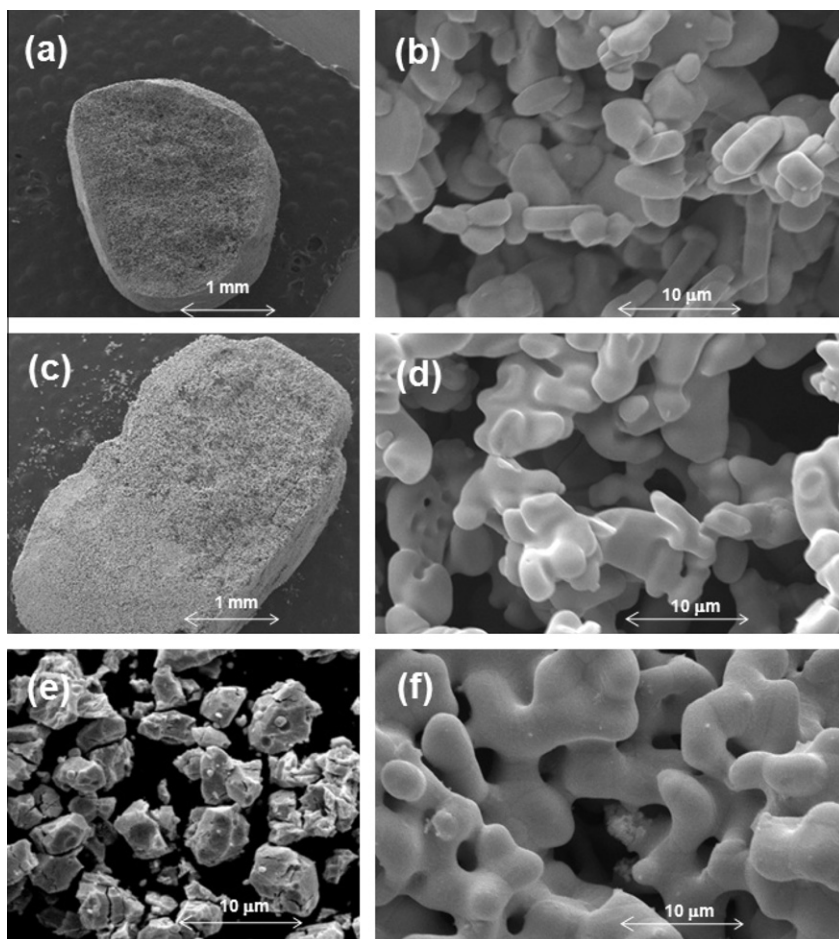


**Fig. 3.** SEM images of the SIMFUEL: low-magnification view (20 $\times$ ) (a) and high-magnification view (3000 $\times$ ), (b) before 4%-H<sub>2</sub>/Ar treatment at 1200 °C; low-magnification view (20 $\times$ ), (c) and high-magnification view (3000 $\times$ ), (d) after 4%-H<sub>2</sub>/Ar treatment at 1200 °C; (e) SIMFUEL powder (3000 $\times$ ), and (f) electrochemically reduced SIMFUEL particles (3000 $\times$ ).

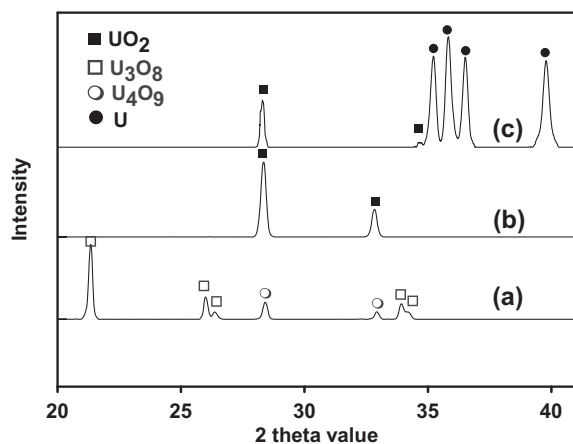


**Fig. 4.** X-ray diffraction patterns of the prepared particles before (a) and after (b) 4%-H<sub>2</sub>/Ar treatment at 1200 °C and (c) after electrochemical reduction.

(b') related to the formation of oxygen gas (b) and the cathodic wave takes place according to reaction (2). In a higher potential range up to 2.42 V, the anodic current of b reaches its maximum value and then decreases due to the depletion of oxide ions near the electrode. At a higher potential than 2.36 V, the anodic current (c) starts to increase again due to the dissolution of platinum:



A cathodic wave (d') appeared in the reverse scan, which is likely due to the reduction of the platinum oxide which formed during the platinum dissolution process in the presence of oxide ion [25].

Fig. 5c shows the CV curves at various scan rates taken to determine the diffusion coefficient of oxide ions. The redox couple of a and a' corresponds to the formation of oxide according to reaction (4). The anodic current density (b) according to reaction (2) increased with an increase in the scan rate. This was in good agreement with the square root of the scan rate as shown in Fig. 5d. The diffusion coefficient,  $D$ , of oxide ions in the LiCl molten salt at 650 °C was calculated to be  $3.16 \times 10^{-5} \text{ cm}^2/\text{s}$  by means of the following equation [26]:

$$I_p = 0.4463 \left( \frac{F^3}{RT} \right)^{1/2} n^{3/2} A D^{1/2} C v^{1/2} \quad (6)$$

Here,  $i_p$  is the peak current (A),  $F$  is the Faraday constant (96,485 C/mol),  $R$  is the gas constant (8.314 J mol/K),  $T$  is the absolute temperature (K),  $n$  is the stoichiometric number of electrons involved in the electrode reaction,  $A$  is the surface area of the electrode,  $C$  is the concentration of oxide ion and  $v$  is the scan rate (V/s). The calculated diffusion coefficient in this work shows a value similar to

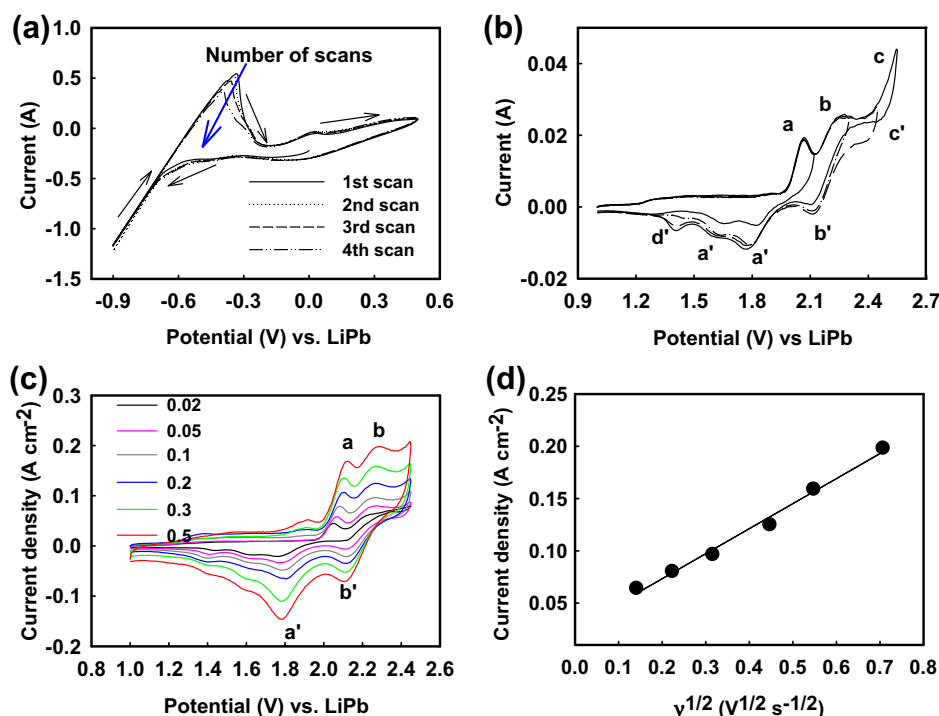


**Fig. 5.** Cyclic voltammograms of (a) a porous SIMFUEL particle in LiCl containing 1 wt.% Li<sub>2</sub>O at 650 °C. Scan rate: 50 mV s<sup>-1</sup>, (b) platinum wire electrode in a LiCl melt at 650 °C. Li<sub>2</sub>O concentration: 0.2 wt.%; scan rate: 50 mV s<sup>-1</sup>, (c) platinum wire electrode in a LiCl melt while varying the scan rate (V/s), and (d) plot of the anodic peak current density vs. the square root of the scan rate. Li<sub>2</sub>O concentration: 0.2 wt.%.

that in previous data derived based on the concentration change [27].

### 3.3. Electrochemical reduction of porous SIMFUEL particles

Fig. 6 shows the response current (b) and cathode potential (c) curves against the applied cell voltage (a) in the electrochemical reduction of 4.1 g of the porous SIMFUEL particles prepared in this work. The cell voltage was stepped down from 3.2 to 3.0 V to suppress the excessive formation of lithium metal while 250% of the theoretical charge necessary for complete reduction was supplied. The response current from 4 to 2.5 A passes through the circuit at the given cell voltages. The spike of the current at each set may be caused by the double-layer charging. The cathode potential was controlled below -0.7 V against Li–Pb, which is cathodic enough to reduce UO<sub>2</sub> to metallic uranium and to reduce Li<sup>+</sup> to Li metal, as observed in the CV result of the SIMFUEL particles (Fig. 5a). The anode potential ranges are in a window between 2.2 and 2.4 V, where the oxidation of the oxide ion mainly takes place to result in an oxygen evolution out of the electrolysis cell [25]. Thus, the metal oxides, including UO<sub>2</sub> as the major component are reduced by reactions (1) and (2). The electrolysis cell was kept in the open circuit condition to avoid the excessive deposition of lithium when the open circuit potential (OCP) exhibits the Li/Li<sup>+</sup> potential (about -0.57 V). As the oxides are converted to the metallic forms, lithium metal may form on the surface of the converted metal in the cathode basket and on its surface. The constant OCP period increased with the reaction time and the OCP eventually remained constant at the Li/Li<sup>+</sup> potential for a long time, indicating the end-point of the run [14,23].

After the electrolysis run finished and the cathode basket was taken out, we observed that the shape of the porous SIMFUEL particles in the cathode basket was unchanged. Cutting was then done along the radial direction in an argon filled glove box. As shown in the inset image of Fig. 6, the reduced SIMFUEL particles gave a

metallic gray color whereas original color was brown before the electrochemical reduction. The sampled particles were analyzed to determine their structure and reduction extent. Fig. 3f shows that the microstructure of the reduced SIMFUEL particles is nodular. In the XRD pattern of the reduced porous SIMFUEL particles (Fig. 4c) the characteristics of metallic U (Fig. 4c) are identified, indicating that the UO<sub>2</sub> contained in the SIMFUEL was successfully converted to metallic U via the electrochemical reduction process. It appears that the peaks corresponding to UO<sub>2</sub> in Fig. 4c appeared due to the partially remaining UO<sub>2</sub> and the re-oxidation during the methanol washing process for the removal of the salt.

Table 2 summarizes the reduction extents for each element after electrolysis. Electrolysis of the porous SIMFUEL particles in which 150% of the theoretical charge was supplied was run in a similar manner to the run presented in Fig. 6. The analysis results are compared in Table 2. In general, the metal portion increases and the metal oxides portion decreases when more charges are supplied to the fuel. Particularly, when 250% of the theoretical charge was introduced to the electrolysis cell, most of the uranium oxide was converted to the metallic form, exhibiting a very high reduction extent of 99.6%. It should be noted that a 150% charge was sufficient for a complete conversion to metal when only uranium oxide was reduced without adding any other metal oxides in previous work by the authors [23]. A possible explanation for the supply of this additional charge would be that the unreduced metal oxides hinder the reduction of uranium oxide [28]. Noble metals oxides except zirconium oxide were converted to the metal phase, showing a high reduction extent. The reason that the extent of metallic Mo slightly decreased in spite of the supply of more charges is probably due to the high volatility of molybdenum oxides. Nonetheless, we believe that molybdenum oxide was comparably reduced by the supply of 150% of the theoretical charge. On the other hand, the reduction of zirconium was less significant, as reported in a previous publication [22]. In contrast to uranium oxide and noble metal oxides except zirconium oxide, rare earth

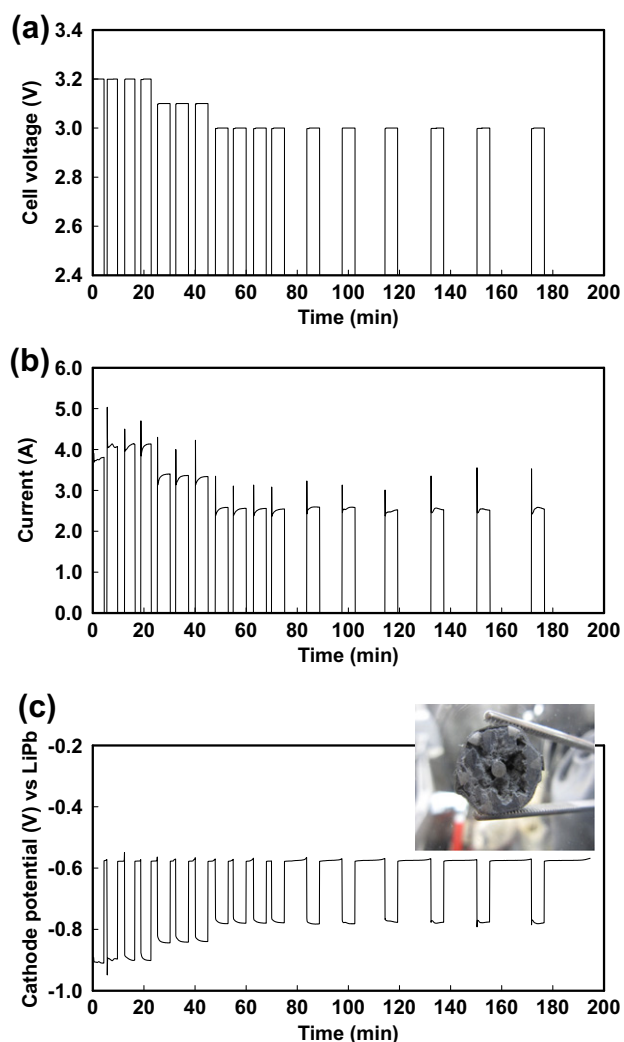


Fig. 6. (a) Cell voltage–time, (b) current–time, and (c) cathode potential–time plots obtained during the electrolysis of porous SIMFUEL particles (4.1 g) in 1 wt.% Li<sub>2</sub>O/LiCl molten salt at 650 °C.

Table 2  
Post-analysis result of the electrochemically reduced SIMFUEL particles.

Supplied charge <sup>a</sup> (%)	Fuel (%)	Elements									
		Rare earth					Noble metal				
		U	Nd	Y	La	Ce	Zr	Mo	Ru	Pd	Rh
150	Metal (%)	88	6	6	4	5	7	83	36	77	58
	Oxide (%)	12	94	94	96	95	93	17	64	23	42
250	Metal (%)	99.6	53	74	50	51	55	78	86	100	67
	Oxide (%)	0.4	47	26	50	49	45	22	14	-	33

<sup>a</sup> Supplied charge (%) to the theoretical value for the complete reduction of the SIMFUEL particle.

oxides exhibit poor reducibility. Some rare earth oxides such as terbium have been successfully reduced by the electrochemical reduction in a pure CaCl<sub>2</sub> melt [29,30]. However, it is not surprising that the rare earth oxides are hardly reduced in this work because Y, Nd, La and Ce metals react with Li<sub>2</sub>O dissolved in LiCl to give their oxides and lithium metal in the 1 wt.% Li<sub>2</sub>O condition according to the thermodynamic calculation [31].

Thus, we consider that actinide and noble metal oxides in an oxide mixture such as the SIMFUEL particles and spent oxide fuel are electrochemically reduced earlier than the rare earth oxides. Afterward, the rare earth oxides confined by the reduced metallic structure may start to be reduced. Herrmann et al. [22] demonstrated the electrochemical reduction of spent light water reactor fuel. They used spent fuel after crushing and sieving it into particles in the range of 45 m–4 mm. A chemical analysis of the reduced spent fuel revealed that the reduction extent of the rare earth oxides was very low. For example, the portions of the Nd, Y, La and Ce oxides were 92%, >81%, >89% and >90%, respectively. In contrast, our results show that the portions of the Nd, Y, La and Ce oxides were only 47%, 26%, 50% and 49% when 250% of the theoretical charge was introduced, respectively, as listed in Table 2. We consider that the reduction extents of the rare earth elements showed marked improvement due to the porous structure of the SIMFUEL particles prepared at a high temperature. The electrochemical reduction of porous oxide proceeds through the propagation of the three-phase interline between the metal, oxide and molten salt phases. The rare earth constituents could be networked with the UO<sub>2</sub> phase to form mixed oxides or solid solutions during the preparation process, which most likely leads to high reducibility of the rare earth oxides [32]. A larger porosity of the SIMFUEL may lead to faster propagation of the three-phase interline due to a decrease in the diffusion resistance inside the solid particle, which may then allow the high-speed electrochemical reduction of the oxide fuel. Also, the highly porous structure of the SIMFUEL particles would be helpful to achieve such a high reduction extent of each element because the electrolyte can easily access to the three-phase interline through the pore and the oxide ions produced from the reduced metal oxide can diffuse faster to the electrolyte bulk.

#### 4. Conclusions

Porous SIMFUEL particles were prepared and electrolyzed to the metallic form. The prepared particles had a highly porous and a well-sintered structure. The porosity of the particles was found to be 70.7%. The cathodic and anodic behaviors during the electrochemical reduction of the SIMFUEL particles were observed by means of CV measurements. Reduction of the SIMFUEL took place at a potential of  $-0.49$  V vs. LiPb. The diffusion coefficient of oxide ions in LiCl molten salt at 650 °C was determined to be  $3.16 \times 10^{-5}$  cm<sup>2</sup>/s. After the electrochemical reduction process, the post-analysis result suggests a very high reduction extent of uranium oxide of 99.6% during the electrochemical reduction of the SIMFUEL particles. Also, a considerable amount of rare earth oxides was reduced to their metallic form due to the sintered and porous structure of the particles. The highly porous structure of the SIMFUEL particles is advantageous to speed up the electrochemical reduction process for pyroprocessing.

#### Acknowledgements

This work was supported by the Nuclear Research & Development Program of the Korea Science and Engineering Foundation grant funded by the Korean government (MEST). Also, this work was partly supported by the Technology Innovation Program funded by the Ministry of Knowledge Economy (MKE, Korea).

#### References

- [1] J.J. Laidler, J.E. Battles, W.E. Miller, J.P. Ackerman, E.L. Carls, Development of pyroprocessing technology, Prog. Nucl. Energy 31 (1997) 131–140.
- [2] R.W. Benedict, H.F. McFarlane, EBR-II spent fuel treatment demonstration project status, Radwaste Mag. 5 (1998) 23.
- [3] M. Iizuka, Y. Sakamura, T. Inoue, Development of pyroprocessing and its future direction, Nucl. Eng. Technol. 40 (2008) 183–190.

- [4] M.F. Simpson, S.D. Herrmann, Modeling the pyrochemical reduction of spent  $\text{UO}_2$  fuel in a pilot-scale reactor, *Nucl. Technol.* 162 (2008) 179–183.
- [5] J.-H. Yoo, C.-S. Seo, E.-H. Kim, H. Lee, A conceptual study of pyroprocessing for recovering actinides from spent oxide fuels, *Nucl. Eng. Technol.* 40 (2008) 581–592.
- [6] S. Kitawaki, T. Shinozaki, M. Fukushima, T. Usami, N. Yahagi, M. Kurata, Recovery of U-Pu alloy from MOX using pyroprocess series, *Nucl. Technol.* 162 (2008) 118–123.
- [7] J. Serp, R.J.M. Konings, R. Malmbeck, J. Rebizant, C. Scheppeler, J.-P. Glatz, Electrochemical behavior of plutonium ion in LiCl–KCl eutectic melts, *J. Electroanal. Chem.* 561 (2004) 143–148.
- [8] J.L. Willit, W.E. Miller, J.E. Battles, Electrorefining of uranium and plutonium – a literature review, *J. Nucl. Mater.* 195 (1992) 229–249.
- [9] S.M. Jeong, S.-B. Park, S.-S. Hong, C.-S. Seo, S.-W. Park, Electrolytic production of metallic uranium from  $\text{U}_3\text{O}_8$  in a 20 kg-batch scale reactor, *J. Radioanal. Nucl. Chem.* 268 (2006) 349–356.
- [10] S.B. Park, B.H. Park, S.M. Jeong, J.M. Hur, C.-S. Seo, S.-H. Choi, S.W. Park, Characteristics of an integrated cathode assembly for the electrolytic reduction of uranium oxide in a LiCl– $\text{Li}_2\text{O}$  molten salt, *J. Radioanal. Nucl. Chem.* 268 (2006) 489–495.
- [11] J.-M. Hur, T.-J. Kim, I.-K. Choi, J.B. Do, S.-S. Hong, C.-S. Seo, Chemical behavior of fission products in the petrochemical process, *Nucl. Technol.* 162 (2008) 192–198.
- [12] G.Z. Chen, D.J. Fray, T.W. Farthing, Direct electrochemical reduction of titanium dioxide to titanium in molten calcium chloride, *Nature* 407 (2000) 361–364.
- [13] Y. Sakamura, M. Kurata, T. Inoue, Electrochemical reduction of  $\text{UO}_2$  in molten  $\text{CaCl}_2$  or LiCl, *J. Electrochem. Soc.* 153 (2006) D31–D39.
- [14] Y. Sakamura, T. Omori, T. Inoue, Application of electrochemical reduction to produce metal fuel material from actinide oxides, *Nucl. Technol.* 162 (2008) 169–178.
- [15] J.-H. Hur, S.M. Jeong, H. Lee, Underpotential deposition of Li in a molten LiCl– $\text{Li}_2\text{O}$  electrolyte for the electrochemical reduction of U from uranium oxides, *Electrochem. Commun.* 12 (2010) 706–709.
- [16] E. Gordo, G.Z. Chen, D.J. Fray, Toward optimisation of electrolytic reduction of solid chromium oxide to chromium powder in molten chloride salts, *Electrochim. Acta* 49 (2004) 2195–2208.
- [17] G.Z. Chen, E. Gordo, D.J. Fray, Direct electrolytic preparation of chromium powder, *Metall. Mater. Trans. B* 35B (2004) 223–233.
- [18] Y. Sakamura, T. Omori, Electrolytic reduction and electrorefining of uranium to develop pyrochemical reprocessing of oxide fuels, *Nucl. Technol.* 171 (2010) 266–275.
- [19] E.-Y. Choi, J.-M. Hur, I.-K. Choi, S.G. Kwon, D.-S. Kang, S.S. Hong, H.-S. Shin, M.A. Yoo, S.M. Jeong, Electrochemical reduction of porous 17 kg uranium oxide pellets by selection of an optimal cathode/anode surface area ratio, *J. Nucl. Mater.* 418 (2011) 87–92.
- [20] J.J. Park, J.W. Lee, J.M. Shin, G.I. Park, K.C. Song, J.W. Lee, An advanced voloxidation process at KAERI, in: *Proc. Global, Paris, France 2009*, pp. 9161.
- [21] G.I. Park, J.W. Lee, J.W. Lee, Y.W. Lee, K.C. Song, Effect of impurities on the microstructure of DUPIC fuel pellets using the SIMFUEL technique, *Nucl. Eng. Technol.* 40 (2008) 1–8.
- [22] S. Herrmann, S. Li, M. Simpson, Electrolytic reduction of spent light water reactor fuel: bench-scale experiment results, *J. Nucl. Sci. Technol.* 44 (2007) 361–367.
- [23] S.M. Jeong, H.S. Shin, S.S. Hong, J.M. Hur, J.B. Do, H.S. Lee, Electrochemical reduction behavior of  $\text{U}_3\text{O}_8$  powder in a LiCl molten salt, *Electrochim. Acta* 55 (2010) 1749–1755.
- [24] H.S. Shin, J.M. Hur, S.M. Jeong, K.Y. Jung, Direct electrochemical reduction of titanium dioxide in molten lithium chloride, *J. Ind. Eng. Chem.* 18 (2012) 438–442.
- [25] S.M. Jeong, H.S. Shin, S.H. Cho, J.M. Hur, H.S. Lee, Electrochemical behavior of a platinum anode for reduction of uranium oxide in a LiCl molten salt, *Electrochim. Acta* 54 (2009) 6335–6340.
- [26] A.J. Bard, L.R. Faulker, *Electrochemical Methods Fundamentals and Applications*, second ed., John Wiley & Sons, 2001.
- [27] Y. Sakamura, Effect of alkali and alkaline-earth chloride addition on electrolytic reduction of  $\text{UO}_2$  in LiCl salt bath, *J. Nucl. Mater.* 412 (2011) 177–183.
- [28] S.M. Jeong, B.H. Park, J.M. Hur, C.S. Seo, H. Lee, K.-C. Song, An experimental study on an electrochemical reduction of an oxide mixture in the advanced spent-fuel conditioning process, *Nucl. Eng. Technol.* 42 (2010) 183–192.
- [29] D. Wang, G. Qiu, X. Jin, X. Hu, G.Z. Chen, Electrochemical metallization of solid terbium oxide, *Angew. Chem. Int. Ed.* 45 (2006) 2384–2388.
- [30] G. Qiu, D. Wang, X. Jin, G.Z. Chen, A direct electrochemical route from oxide precursors to the terbium–nickel intermetallic compound  $\text{TbNi}_5$ , *Electrochim. Acta* 51 (2006) 5785–5793.
- [31] B.H. Park, S.B. Park, S.M. Jeong, C.S. Seo, S.W. Park, Electrolytic reduction of spent oxide fuel in a molten LiCl– $\text{Li}_2\text{O}$  system, *J. Radioanal. Nucl. Chem.* 270 (2006) 575–583.
- [32] L.A. Barnes, M.A. Williamson, Electrolytic reduction of uranium oxide containing rare earth oxide fission product, in: *International Pyroprocessing Research Conference, Jeju Island, Korea, August 24–27, 2008*, pp. 94–95.